WIFI-BASED ROBUST CHILD PRESENCE DETECTION FOR SMART CARS

Sakila S. Jayaweera, *Beibei Wang†, Xiaolu Zeng†, Wei-Hsiang Wang†*, K. J. Ray Liu†*

†Origin Wireless Inc., *University of Maryland

ABSTRACT

In-car child presence detection (CPD) has gained worldwide attention due to increased child deaths reported yearly when they are left unattended in a car. Existing solutions usually require dedicated sensors and are being surpassed by WiFi-based CPD because the latter can provide broader coverage and can reuse the in-car WiFi devices. However, the existing WiFi-based CPD solutions are not robust and may suffer from miss detection due to the very weak breathing of a young child and high false alarms under unfavorable environmental conditions. In this paper, we propose a WiFi-based robust CPD system consisting of a motion and breathing detector. To improve breathing detection, we propose to treat the intermediate spectrogram for breathing estimation as images and apply image enhancement techniques followed by effective false alarm removal. Extensive experimental results have confirmed the robustness of the proposed system with a 99% detection accuracy and 3% false alarm rate.

Index Terms— WiFi sensing, channel state information (CSI), child presence detection (CPD)

1. INTRODUCTION

In-car child presence detection (CPD) has gained attention from all over the world due to an increasing number of heatstroke child deaths/hypothermia cases when they are left unattended inside a car. Earlier CPD solutions mainly utilize various types of sensor measurements such as those from optical/weight/heat/pressure sensors [1], capacitive sensors [2], and PIR sensors [3]. However, these approaches usually can only provide limited coverage while suffering from a high false alarm rate. Camera-based CPD systems have better detection accuracy, but they heavily rely on the quality of the captured images/videos and are thus vulnerable to poor light conditions [4], [5]. Recent years have witnessed more in-vehicle sensing systems based on radio frequency (RF) signals, such as vital sign detection [6], [7] because RF-based sensing is less privacy intrusive and easy to install [8–12]. But these systems mostly rely on mmWave signals with limited coverage only in their field of view, and mmWave is not readily available in most vehicles today either.

With the ubiquitous deployment of WiFi, more and more vehicles today already/will have WiFi equipment, and thus CPD can reuse the in-car WiFi at no additional cost [13], [14]. A highly accurate and fast-responsive WiFi-based CPD has been proposed in [15], [16] that can offer a large coverage with no calibration efforts. However, its performance has not been fully tested against unfavorable environmental conditions, such as when there exists interfering motion from around the car or under bad weather (e.g., heavy rain), which are practical but non-trivial challenges.

To improve the CPD performance resilient to aforementioned environmental interference, we proposed a robust CPD solution with enhanced vital sign (breathing) detection. We first model the channel state information (CSI) based on statistical electromagnetic (EM) wave theory and utilize an autocorrelation function (ACF) of the CSI to fully leverage all the multipath components [15, 17–19]. We then define a motion detector with a statistic metric to quantify the motion intensity and further define a breathing detector with maximal ratio combining (MRC)-based subcarrier selection to boost the signal-to-noise (SNR) ratio of the ACF, where the weight is the motion intensity in each subcarrier. Even though the CPD solution [15] can achieve good detection in many test cases, it will fail in some cases with very subtle breathing movement, especially under outside motion interference, and one such example is shown in Fig. 1 where Fig. 1 (a) depicts the corrupted ACF due to the outside heavy rain while a child is sleeping (breathing without any motion) inside the car.

Considering that the breathing detection is essentially equivalent to identifying the pattern (horizontal breathing traces) from the ACF spectrogram, we propose to treat the ACF spectrogram as an image, and further improve its SNR with image enhancement techniques and an enhanced ACF spectrogram example is shown in Fig. 1 (b). While enhancement improves the detection of weak breathing under interference, it may also increase the false alarm rates as the non-breathing spectrogram after enhancement may also result in breathing-like patterns, and thus we leverage a zero crossing rate (ZCR) and Dynamic Time Warping (DTW) distance measures to remove such false alarms. To validate the performance of the proposed system, extensive experiments are conducted using a baby doll and real babies under challenging conditions, such as with heavy rain, wind, and when

(a) Corrupted ACF

(b) Enhanced ACF
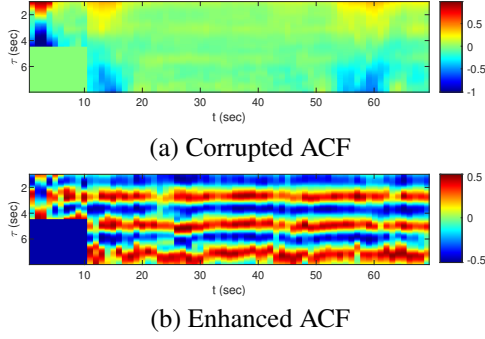
Fig. 1. Improved ACF using the proposed method.

Fig. 2. Robust CPD system design

the car is parked in a busy parking lot. The proposed CPD system demonstrates a 99% detection accuracy and about 3% false alarm rate with challenging data.

The rest of the paper is organized as follows. Section 2 introduces the CSI multi-path model. The system design is presented in Section 3 followed by the experimental results and evaluation in Section 4. Section 5 concludes the paper.

2. CSI MODEL

In an environment with rich multi-path propagation, such as inside a car, WiFi signals can be reflected, scattered, and diffracted by human bodies, seats, floors, or vehicle bodies before arriving at the receiver. Due to the above effect, hundreds of multi-path components (MPC) are superimposed at the receiver. Dynamic objects like the human body may create time-variant MPC while static targets create time-invariant MPC. Even a static human may create time-variant MPC as WiFi is sensitive to the periodic abdomen or chest movement due to breathing. Considering the multi-path effect, the CSI estimated over a subcarrier with frequency f at time t from the received signal can be modeled as

$$H(t, f) = \sum_{m \in \Omega_s} a_m(t) e^{-j2\pi f \tau_m(t)}$$
$$+ \sum_{n \in \Omega_d} a_n(t) e^{-j2\pi f \tau_n(t)} + n(t, f), \quad (1)$$

where $n(t, f)$ is the measurement noise, $a_m(t), a_n(t)$ are the complex amplitudes, τ_m, τ_n are the time delay of the m and n-th multipath components, and Ω_s, Ω_d denotes the time-invariant and time-variant multi-path components, respectively. Without loss of generality, the static multi-path components' complex amplitude and time delay can be assumed as a constant, and thus

$$H(t, f) = H_s(f) + \sum_{n \in \Omega_d} a_n(t) e^{-j2\pi f \tau_n(t)} + n(t, f). \quad (2)$$

In practice, the CSI phase can be corrupted by time and frequency synchronization offsets. Thus, in our statistical

model, we consider the power response of $H(t, f)$ which can be given as

$$G(t, f) = |H(t, f)|^2 = \mu(t, f) + \epsilon(t, f), \quad (3)$$

where $\mu(t, f) = |H_s(f) + \sum_{n \in \Omega_d} a_n(t) e^{-j2\pi f \tau_n(t)}|^2$ and $\epsilon(t, f)$ is the power of the measurement noise $n(t, f)$ which can be modeled as additive white Gaussian noise (AWGN) [17].

3. SYSTEM DESIGN

The proposed CPD system consists of two detector modules: a motion detector and a breathing detector. As illustrated in Fig. 2, the extracted CSI is first fed into the motion detector to detect a child who is awake and may have substantial motion. If there is not a strong enough motion detected, e.g., when a child falls asleep and keeps stationary, the CSI is further fed into the breathing detector to detect potential breathing signals. CPD is triggered if either of the two detectors detects the child's presence by motion or breathing.

3.1. Motion Detector

The motion detector evaluates the motion intensity through motion statistics which is first introduced in our earlier work [17] for indoor motion sensing. It is found that the ACF of the CSI power can well characterize the motion of the surrounding dynamic scatterers, as given by

$$\rho_G(\tau, f) = \frac{\text{cov}[G(t, f), G(t + \tau, f)]}{\text{var}[G(t, f)]} \quad (4)$$

$$= \frac{E_d^2(f)}{E_d^2(f) + \sigma^2(f)} \rho_\mu(\tau, f) + \frac{\sigma^2(f)}{E_d^2(f) + \sigma^2(f)} \delta(\tau), \quad (5)$$

where $E_d^2(f)$ is the power of dynamic scatters, $\rho_\mu(\tau, f)$ is auto-correlation of $\mu(t, f)$, $\sigma^2(f)$ is the variance of $\epsilon(t, f)$, and $\delta(\tau)$ is the Dirac delta function. When $\tau \to 0$, if there is a motion, $\rho_G(\tau, f) \to \frac{E_d^2(f)}{E_d^2(f) + \sigma^2(f)} > 0$; if there is no motion,

$\rho_G(\tau, f) = 0$ since $E_d^2(f) = 0$. Thus, $\lim_{\tau \to 0} \rho_G(\tau, f)$ can be considered as good statistic to measure motion. In practise, $\lim_{\tau \to 0} \rho_G(\tau, f)$ can be approximated by $\rho_G(\tau = 1/F_s, f)$, where F_s is the sampling frequency, and the **motion statistics** is defined as $\psi = \frac{1}{F} \sum_{f=1}^{F} \rho_G(\tau = 1/Fs, f)$, where F denote the set of all sub-carriers.

3.2. Breathing Detector

Since the breathing motion is mainly caused by the periodic chest and abdomen movement, it can be detected by estimating the periodicity from the CSI or the ACF in (5), which also exhibits periodic breathing patterns [19]. As the breathing motion of a child is more subtle than that of an adult, a maximal ratio combining (MRC)-based approach can be adopted to boost the SNR of the ACF, where the top N subcarriers based on the largest motion statistics are selected, and the boosted ACF can be expressed as

$$\hat{\rho}_c(\tau) = \sum_{i=1}^{N} \rho_G(\tau = 1/F_s, f_i)\rho_G(\tau, f_i), \qquad (6)$$

and the breathing rate can be estimated by $f_B = 60/\hat{\tau}$ (BPM), where $\hat{\tau}$ corresponds to the time lag of the first peak in $\hat{\rho}_c(\tau)$.

3.2.1. Enhancement on ACF

Although [15] has utilized the boosted ACF $\hat{\rho}_c(\tau)$ to detect breathing for CPD, we notice miss detection when the ACF is corrupted due to interference motion, as seen from an example of the ACF at a certain time instance in Fig. 3(a), which corresponds to a static child breathing quietly inside a car while raining outside.

Since the breathing detection is, in essence, to identify the peaks in $\hat{\rho}_c(\tau)$, if we have observed the ACF $\hat{\rho}_c(\tau)$ in a certain time window, it boils down to identifying the pattern, i.e., horizontal breathing traces from the ACF. Thus, we propose to view the ACF spectrogram as a 2D image and further improve its SNR with enhancement techniques to restore the breathing traces corrupted by noise/interference.

First, a median filter in the time domain can be applied to remove high-frequency components. Then, edge detection/enhancement can be used in the vertical direction to enhance the horizontal stripes, which can reflect the breathing periodicity. In this paper, we utilize a 1D column filter. For a given time instance t, the enhanced ACF $\hat{\rho}_E(\tau)$ can be given as, $\hat{\rho}_E(\tau) = \hat{\rho}_c(\tau) + k\hat{\rho}_c'(\tau)$, where $\hat{\rho}_c'(\tau)$ is the first derivative of the boosted ACF $\hat{\rho}_c(\tau)$ in (6) and k is a weighting factor. The enhanced ACF with more prominent peaks in the example of Fig. 3(a) is shown in Fig. 3(b).

After peak enhancement, histogram equalization [20] can be further applied to the ACF to adjust and enhance the contrast of the spectrogram for better identification. An example with both enhancements to improve the ACF spectrum is as depicted in Fig. 1.
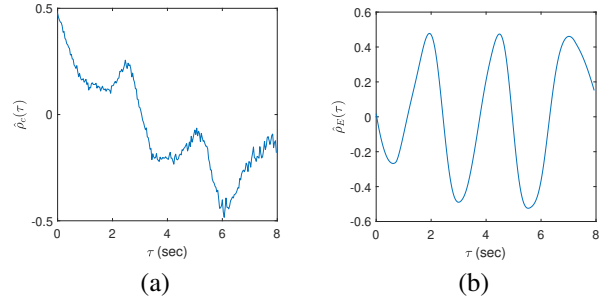
Fig. 3. Example of (a) corrupted ACF, and (b) ACF after peak enhancement.
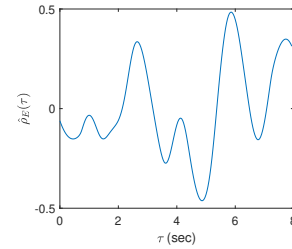
Fig. 4. Fallacious periodic pattern

3.2.2. False alarm removal

Even though motions outside a car may not create high enough motion statistics and trigger motion detection, some such motion can illustrate periodic patterns in the ACF even when the car is empty, which may even be further magnified after the enhancement step and trigger false breathing detection. To mitigate these false alarms, we propose two metrics to evaluate whether the breathing detection is true positive or not.

Zero Crossing Rate (ZCR): As can be seen in Fig. 3(b), at a certain time instant, if there is a breathing signal present, the ACF will exhibit a clear periodic pattern; if there is no breathing, the noise term will dominate the ACF and we can observe many oscillations in $\hat{\rho}_c(\tau)$, which result in a higher number of zero crossings [21]. Therefore, we use the ZCR as a metric to remove the false breathing detection. If the ZCR is higher than a predefined threshold, the system will not trigger the CPD indicator.

DTW distance: As depicted in Fig. 4, for a given time instant, ACF may exhibit fallacious breathing-like patterns which cannot be removed by checking ZCR. To eliminate this shortcoming, we compare the ACF with a template, which can be predefined based on the average breathing rate of a normal child.

Since the ACF can be out of sync with the template due to phase shift or distortion in time, we use the DTW distance to minimize such effects [22]. When the ACF and the breathing template are similar, i.e., the ACF is more likely from a true
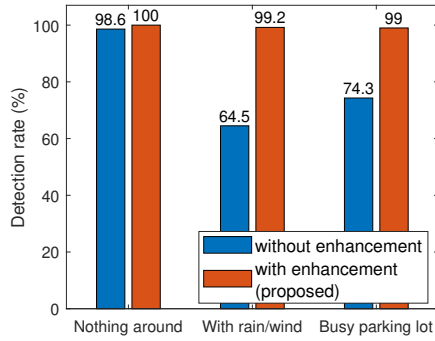
Fig. 5. Detection under different conditions with and without applying the enhancement.

Fig. 6. False alarm rates with and without false alarm removal.

breathing signal, the DTW distance has a smaller value. Thus, the proposed CPD system does not trigger any detection if the DTW distance is higher than a predefined threshold.

After the ACF enhancement and false alarm removal, the proposed CPD system proceeds to peak detection and the breathing rate can be calculated using the average interval of two adjacent peaks.

4. EXPERIMENTAL RESULTS

We implemented our system using a commercial dual-band WiFi module operating in both 2.4GHz and 5GHz bands as in [15], and both the transmitter and the receiver have two omnidirectional antennas. To evaluate the system performance, we use the same dataset as in [15] and expand it with more challenging data from the following cases: 1) severe environmental conditions, such as rain and wind, 2) target car parking in a busy parking lot and 3) large motions around the target car, including periodic walking, hand waving near car windows, and loading/unloading bags from adjacent cars, so as to verify the robustness of the proposed system. Experiments were conducted over a month using different car models, and we have around 100 minutes long data samples for each challenging case. We collected child presence data using a baby doll and children under the age of six with their parents' approval.

4.1. Overall Performance

The overall detection and false alarm rate performance for all the test cases are summarized in Table 1, showing a 99% detection and around 3% false alarm. We also compared the proposed system with WiCPD [15]. Although WiCPD utilizes a transition target detector to detect children in transition status, such as sleeping with minor motions, it cannot address breathing detection under outside interference, and thus the proposed method outperforms WiCPD in overall performance. In addition, the proposed system can detect a static
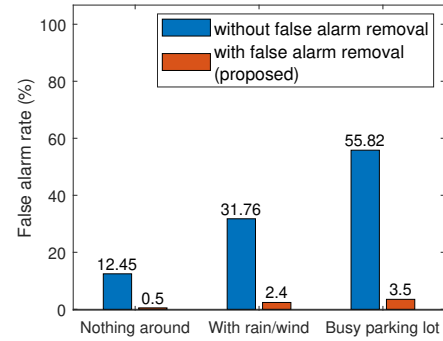
child or child in motion within 10 seconds of responsive time. The detection accuracy and delay performance can well satisfy the Euro NCAP protocol requirements which shows its great potential for commercial applications.

Table 1. Results comparison

	Detection accuracy	False alarm rate
WiCPD [15]	82.4%	6.6%
Proposed method	99.0%	3.2%

4.2. Benchmark Study

Fig. 5 evaluates the performance of the proposed CPD system with and without applying the enhancement on ACF. When there is "Nothing around", meaning there is no motion or interference outside the car, both methods perform well, while with the proposed enhancement, the detection accuracy increases to 99.2% with rain/wind and 99% in a busy parking lot. Further depicted in Fig. 6, the proposed CPD system achieves a lower false alarm rate in every scenario with the false alarm removal techniques.

5. CONCLUSION

This paper presents a robust WiFi-based CPD system that is resilient to interference such as outside motion or bad weather conditions. The proposed CPD system consists of a motion detector and a breathing detector. Breathing detection is improved by applying image enhancement on the intermediate spectrogram, followed by false alarm removal. The experimental results show that the implemented CPD system can achieve 99% detection accuracy and 3% false alarm rate even under unfavorable environmental conditions with less than 10s response time.

6. REFERENCES

[1] K. N. Khamil, S. Rahman, and M. Gambilok, "Babycare alert system for prevention of child left in a parked vehicle," *ARPN Journal of Engineering and Applied Sciences*, vol. 10, no. 22, pp. 17313–17319, 2015.

[2] A. Ranjan and B. George, "A child-left-behind warning system based on capacitive sensing principle," in *2013 IEEE International Instrumentation and Measurement Technology Conference (I2MTC)*. IEEE, 2013, pp. 702–706.

[3] N. Hashim, H. Basri, A. Jaafar, M. Aziz, A. Salleh, and A. S. Ja, "Child in car alarm system using various sensors," *ARPN Journal of Engineering and Applied Sciences*, vol. 9, no. 9, pp. 1653–1658, 2014.

[4] C. Fan, Y. Wang, and C. Huang, "Heterogeneous information fusion and visualization for a large-scale intelligent video surveillance system," *IEEE transactions on systems, man, and cybernetics: systems*, vol. 47, no. 4, pp. 593–604, 2016.

[5] J. Jaworek-Korjakowska, A. Kostuch, and P. Skruch, "SafeSO: Interpretable and explainable deep learning approach for seat occupancy classification in vehicle interior," in *2021 IEEE/CVF Conference on Computer Vision and Pattern Recognition Workshops (CVPRW)*, 2021, pp. 103–112.

[6] F. Wang, X. Zeng, C. Wu, B. Wang, and K. J. R. Liu, "mmhrv: Contactless heart rate variability monitoring using millimeter-wave radio," *IEEE Internet of Things Journal*, vol. 8, no. 22, pp. 16623–16636, 2021.

[7] F. Wang, X. Zeng, C. Wu, B. Wang, and K. J. R. Liu, "Driver vital signs monitoring using millimeter wave radio," *IEEE Internet of Things Journal*, 2021.

[8] B. Wang, Q. Xu, C. Chen, F. Zhang, and K.J. R. Liu, "The promise of radio analytics: A future paradigm of wireless positioning, tracking, and sensing," *IEEE Signal Processing Magazine*, vol. 35, no. 3, pp. 59–80, 2018.

[9] K. J. R. Liu and B. Wang, *Wireless AI: Wireless Sensing, Positioning, IoT, and Communications*, Cambridge University Press, 2019.

[10] C. Chen, Y. Han, Y. Chen, H. Q. Lai, F. Zhang, B. Wang, and K. J. R. Liu, "TR-BREATH: Time-reversal breathing rate estimation and detection," *IEEE Transactions on Biomedical Engineering*, vol. 65, no. 3, pp. 489–501, 2018.

[11] F. Wang, F. Zhang, C. Wu, B. Wang, and K. J. R. Liu, "Respiration tracking for people counting and recognition," *IEEE Internet of Things Journal*, vol. 7, no. 6, pp. 5233–5245, 2020.

[12] F. Wang, F. Zhang, C. Wu, B. Wang, and K. J. R. Liu, "ViMo: Multiperson vital sign monitoring using commodity millimeter-wave radio," *IEEE Internet of Things Journal*, vol. 8, no. 3, pp. 1294–1307, 2021.

[13] X. Zeng, F. Wang, B. Wang, K. J. R. Wu, C.and Liu, and O. C. Au, "In-vehicle sensing for smart cars," *IEEE Open Journal of Vehicular Technology*, vol. 3, pp. 221–242, 2022.

[14] Q. Xu, B. Wang, F. Zhang, S. D. Regani, F. Wang, and K. J. R. Liu, "Wireless ai in smart car: How smart a car can be?," *IEEE Access*, vol. 8, pp. 55091–55112, 2020.

[15] X. Zeng, B. Wang, C. Wu, S. D. Regani, and K. J. R. Liu, "WiCPD: Wireless child presence detection system for smart cars," *IEEE Internet of Things Journal*, 2022.

[16] X. Zeng, B. Wang, C. Wu, S. D. Regani, and K. J. R. Liu, "Intelligent wi-fi based child presence detection system," in *ICASSP 2022 - 2022 IEEE International Conference on Acoustics, Speech and Signal Processing (ICASSP)*, 2022, pp. 11–15.

[17] F. Zhang, C. Wu, B. Wang, H. Q. Lai, Y. Han, and K. J. R. Liu, "WiDetect: Robust motion detection with a statistical electromagnetic model," *Proceedings of the ACM on Interactive, Mobile, Wearable and Ubiquitous Technologies*, vol. 3, no. 3, pp. 1–24, 2019.

[18] F. Zhang, C. Chen, B. Wang, and K. J. R. Liu, "WiSpeed: A statistical electromagnetic approach for device-free indoor speed estimation," *IEEE Internet of Things Journal*, vol. 5, no. 3, pp. 2163–2177, 2018.

[19] F. Zhang, C. Wu, B. Wang, M. Wu, D. Bugos, H. Zhang, and K. J. R. Liu, "SMARS: Sleep monitoring via ambient radio signals," *IEEE Transactions on Mobile Computing*, vol. 20, no. 1, pp. 217–231, 2019.

[20] T. Acharya and A. K. Ray, *Image processing: principles and applications*, John Wiley & Sons, 2005.

[21] B. Kedem and S. Yakowitz, *Time series analysis by higher order crossings*, IEEE press New York, 1994.

[22] P. Senin, "Dynamic time warping algorithm review," *Information and Computer Science Department University of Hawaii at Manoa Honolulu, USA*, vol. 855, no. 1-23, pp. 40, 2008.